HEMATITE AT MERIDIANI PLANUM, MARS, INVESTIGATED BY SIMULTANEOUS FITTING OF MER MÖSSBAUER SPECTRA. I. Fleischer<sup>1</sup>, D. G. Agresti<sup>2</sup>, G. Klingelhöfer<sup>1</sup> and R. V. Morris<sup>3</sup>, <sup>1</sup>Institut für Anorganische und Analytische Chemie, Johannes-Gutenberg-Universität Mainz, Germany (fleischi@uni-mainz.de), <sup>2</sup>University of Alabama at Birmingham, Birmingham, AL 35294-1170 (agresti@uab.edu), <sup>3</sup>NASA Johnson Space Center, Houston, Texas.

Introduction: The Mars Exploration Rover Opportunity encountered sedimentary outcrop rocks at its landing site. Spherules with diameters in the millimeter range were found to weather from the outcrop rocks. With Opportunity's miniaturised Mössbauer spectrometer MIMOS II, hematite was detected in spherules and in the outcrop matrix [1,2]. Figure 1 shows the target Berry Bowl, where brushed outcrop and an accumulation of spherules could be investigated on sols 46 and 48 of Opportunity's mission.

Hematite undergoes a transition from a weakly ferromagnetic above to an antiferromagnetic state below the Morin temperature ( $T_M \sim 265~K$  for chemically pure, crystalline hematite). The magnetic hyperfine splitting ( $B_{hf}$ ) shows a general decrease with increasing temperature and a drop of  $\sim 0.8~T$  at  $T_M$ . The quadrupole splitting ( $\Delta E_Q$ ) changes its sign at  $T_M$ , with negative values above and positive values below the transition. Crystallinity and particle size influence the magnitude and temperature dependence of the magnetic splitting and the quadrupole splitting [3]. On this basis, Mössbauer spectra may allow to distinguish Meridiani hematite populations with different degrees of crystallinity, different particle sizes and/or impurities.



Figure 1: The target Berry Bowl (Sol 48, Pancam sequence P2568), where brushed outcrop (circular spot) and an accumulation of spherules (to the right of the brushed spot) were investigated.

**Data analysis:** We use simultaneous fitting ("simfitting") to analyse the MER Mössbauer spectra [4,5]. We presented first simfit results in [6], using "one-dimensional" simfitting, where relations were established between separate spectra corresponding to different temperature windows, taken on the same target. Compared to single spectrum fits, this approach provided tighter and more consistent parameter trends, but did not allow to correlate spectra from different targets, taken at the same temperature. Both correlations, by temperature and by target, were implemented

in "two dimensional" simfitting. This approach allowed to establish consistent temperature dependent trends for parameters from separate targets. Furthermore, this method was found to be an effective way to compare different spectral models for Meridiani hematite. We presented results for outcrop hematite in [7].

Spectra were obtained in the temperature range between 190K and 290K, in 10K wide temperature windows [8]. Spectra obtained on the same target and in the same temperature window were summed. We focus on a simfit data set of 60 spectra from outcrop and 46 spectra from spherule targets (10 separate targets each). In addition to hematite, outcrop spectra were modeled with doublets for olivine (Ol), pyroxene (Px), a yet unassigned ferric phase (Fe3D3 [1]) and jarosite (Jar). For Ol and Px, Mössbauer parameters and line widths were constrained to values reported in [1]. For Fe3D3 and Jar, Mössbauer parameters and line widths were set equal for all spectra. Area ratios for all doublets were held equal for spectra from the same target. Apart from hematite, spherule spectra were modeled with doublets for Ol, Px and nanophase ferric oxide (npOx [1]), and two sextets for magnetite (Mt). Doublet parameters and line widths were held equal for all spectra. Mt parameters, line widths, and relative areas of both sextets were constrained to values obtained from a magnetite-rich target encountered by MER-A Spirit (Peace, Sol 379) [9,10]. Area ratios for Ol, Px, npOx and Mt were held equal for spectra from the same target. The hematite in outcrop and spherules was modeled with two separate sextets with lorentzian line shapes, hematite subspectra were modeled with the same area ratio for all subspectra of a given temperature window. We performed fits with separate models that can be distinguished based on line shapes (symmetric or skewed lorentzian lines) and line widths (equal line widths for all six lines of a sextet or broadening from inner to outer lines as ( $\Gamma$ ,  $\Gamma$ +d,  $\Gamma$ +2d)). We use the notation "S1" for the sextet with the larger magnetic hyperfine field (B<sub>hf</sub>), and "S2" for the sextet with the smaller B<sub>hf</sub>.

Results: Simfits with different distributions of line widths yield rather similar results for outcrop and spherule spectra. Here, we summarize general, model-independent results, for which we consider average values from four separate simfits for spherule and outcrop spectra, respectively, modeled with symmetric lorentzian lines for both sextets, and from three separate simfits for outcrop spectra modeled with symmetre

ric lines for S1 and skewed lines for S2. A detailed discussion of results from separate models and differences between them is given in [10].

Figure 2 shows the temperature dependence of  $B_{hf}$  and  $\Delta E_Q$  for outcrop and spherules. Generally, the range of values obtained from different models is considerably smaller for spherules (0.2 T for  $B_{hf}$ ; 0.02 mm/s for  $\Delta E_Q$ ) than for outcrop (0.9 T for  $B_{hf}$ ; 0.1 mm/s for  $\Delta E_Q$ ), presumably because of the larger hematite subspectral area in spherule spectra.

For outcrop and spherules,  $B_{hf}$  shows a slight decrease with increasing temperature.  $B_{hf}(S1)$  is above ~52.5 T and larger than  $B_{hf}(S2)$ , which remains below this value. For outcrop,  $B_{hf}$  is larger by ~1T for models with skewed lines for S2.

The temperature dependence of  $\Delta E_Q$  is substantially different for outcrop and spherules. Values significantly above zero, characteristic for the antiferromagnetic state below the Morin temperature, are only observed for S1 from outcrop, where  $\Delta E_Q$  is ~0.2 mm/s at 205 K, changes sign at ~255K, and decreases to a value of ~ -0.15 mm/s at 275K. For S2 from outcrop and S1 from spherule spectra,  $\Delta E_Q$  is ~0 mm/s at 205K.

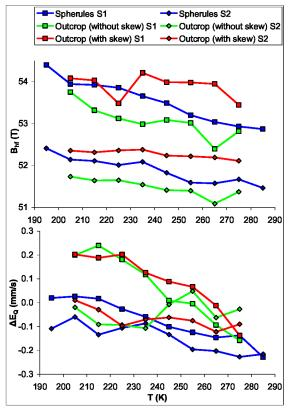


Figure 2: temperature dependence of  $B_{hf}$  and  $\Delta E_Q$  for outcrop and spherules; average values from different models with symmetric lines (spherules and outcrop) and skewed lorentian lines (outcrop).

Outcrop S2 decreases to  $\sim$  -0.15 mm/s at 275 K, both spherule sextets to  $\sim$  -0.2 mm/s at 285 K.

A sudden jump would be expected for  $\Delta E_Q$  for well-crystalline hematite. Instead of this behaviour, we observe a quasilinear decrease with temperature. We also observed this behaviour for natural hematite bearing samples (<1000 $\mu$ m sieve fraction, dominated by much smaller particle sizes), measured with a laboratory copy of the MER instrument at Mars-equivalent temperatures [10].

For all models and all spectra, the Mössbauer center shift  $\delta$  was found to be independent of temperature. The relative areas of the two hematite sextets are ~30% S1 and ~70% S2 for outcrop, and ~65% S1 and ~35% S2 for spherules.

Conclusions: The application of two dimensional simfitting to MER Mössbauer data from Eagle crater enables us to distinguish different hematite populations in the outcrop matrix and in spherules. Figure 3 shows a comparison of our results with values from [1]. For outcrop, S2 overlaps with values from [1]; S1 shows a Morin transition. For spherules, values from [1] are intermediate between S1 and S2. Hematite with clear signatures for the presence of a Morin transition occurs in the outcrop matrix, indicating that well-crystalline material is only present in the outcrop matrix. The Morin transition is suppressed in all other cases, because of low crystallinity or very small particle sizes.

**Acknowledgement:** funded by German Space Agency under contract 50QM9902.

**References:** [1] Morris, R.V., et al. (2006b), *JGR*, 111, E12S15. [2] Klingelhöfer et al. (2004) Science, 306, 1740-1745. [3] E. Murad & J. Cashion, Kluwer Acad. Publishers (2004). [4] Agresti D.G. & Gerakines P.A. (2009) *Hyp. Int.*, 188,113–120. [5] Agresti D.G. et al. (2006) *Hyp. Interact.*, 170, 67–74. [6] Fleischer et al. (2009), *LPS XL*, Abstract #1835. [7] Agresti et al., Journal of Physics, accepted. [8] Klingelhöfer, G., et al. (2003) *JGR 108*, 8067. [9] Morris, R.V., et al. (2006a), *JGR*, 111, E02S13. [10] Fleischer et al., manuscript in preparation.

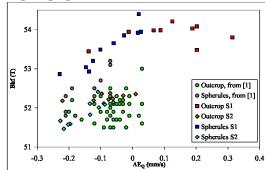


**Figure 3:** Comparison of parameters ( $B_{hf}$  vs.  $\Delta E_Q$ ) from [1] and our fits (average values, with skewed lines for outcrop S2).